Cotunneling and non-equilibrium magnetization in magnetic molecular monolayers

Florian Elste[1,*] and Carsten Timm[2,†]

[1]*Institut für Theoretische Physik, Freie Universität Berlin, Arnimallee 14, 14195 Berlin, Germany*
[2]*Department of Physics and Astronomy, University of Kansas, Lawrence, Kansas 66045, USA*

(Dated: November 4, 2006)

Transport and non-equilibrium magnetization in monolayers of magnetic molecules subject to a bias voltage are considered. We apply a master-equation approach going beyond the sequential-tunneling approximation to study the Coulomb-blockade regime. While the current is very small in this case, the magnetization shows changes of the order of the saturation magnetization for small variations of the bias voltage. Inelastic cotunneling processes manifest themselves as differential-conductance steps, which are accompanied by *much larger* changes in the magnetization. In addition, the magnetization in the Coulomb-blockade regime exhibits strong signatures of sequential tunneling processes *de*-exciting molecular states populated by inelastic cotunneling. We also consider the case of a single molecule, finding that cotunneling processes lead to the occurrence of *magnetic sidebands* below the Coulomb-blockade threshold. In the context of molecular electronics, we study how additional spin relaxation suppresses the fine structure in transport and magnetization.

PACS numbers: 73.63.-b, 75.50.Xx, 85.65.+h, 73.23.Hk

I. INTRODUCTION

The idea of *molecular spintronics* consists of integrating the promising concepts of molecular electronics and spintronics.[1,2,3,4,5,6] A particularly interesting aspect of molecular electronics, besides the prospect of further miniaturization, is the possibility to use chemical synthesis for the fabrication of device components. This bottom-up process would start from relatively simply molecules and be massively parallel. In this context, spintronics is discussed in relation to magnetic memory[7] and quantum computation.[8] Both ideas rely on *magnetic* molecules.[9] Partly for this reason electronic transport through magnetic molecules has recently received a lot of attention.[10,11,12,13,14,15,16,17,18,19,20,21,22,23,24]

Experimental research has focused on the fine structure of the Coulomb-blockade peaks[10,11,16,17] and on Kondo correlations in single-molecule transistors.[10,11,25] Furthermore, novel spin-blockade mechanisms and negative differential conductance have been observed.[16,17] These findings have also stimulated theoretical work, which mostly employs the sequential-tunneling approximation.[13,14,15,18,19,20,21,22,23] Like artificial quantum dots, a molecular junction is in the Coulomb-blockade regime at sufficiently small bias voltage, except at crossing points where two states with electron numbers differing by unity become degenerate. Due to the discreteness of molecular many-particle energies for weak coupling to the leads, there are typically no molecular transition energies in the window between the chemical potentials of the leads for small bias. In this regime the very small tunneling current is not correctly described by the sequential-tunneling approximation. It is instead dominated by *cotunneling*, which appears in fourth order in the perturbation expansion in the tunneling amplitude. However, despite its experimental observation,[17] transport through magnetic molecules in this regime has been little studied.[24]

We study magnetic molecules under a bias voltage in the Coulomb-blockade regime. Our main result is that while any features in the differential conductance are very small due to the suppression of the current, there are *large* changes in the average magnetic moments of the molecules with bias voltage and applied field. The measurement of magnetic moments of sub-monolayers of molecules has been demonstrated 20 years ago.[26] Even the detection of the spin of a single molecule may be feasible.[27,28] However, it is not clear how to perform such a measurement in a break-junction experiment. We here mainly consider a *monolayer* of magnetic molecules between metallic electrodes, since the measurement of the magnetization of a thin film is expected to be easier than of a single molecule. Note that various molecules form nearly perfect monolayers on metallic substrates.[29]

To find the current and the non-equilibrium magnetization, we use the master-equation formalism, treating the tunneling to the leads as a perturbation.[13,18,19,30,31,32] This approach describes the Coulomb and exchange interactions on the molecule *exactly* and works also far from equilibrium. In particular, it is not restricted to the linear-response regime of small bias voltage.

For memory applications the control of spin relaxation is crucial. Since cotunneling and additional spin relaxation due to, e.g., dipolar and hyperfine interactions, have similar selection rules for molecular transitions, consistency requires to include both. We find that spin relaxation is very effective in washing out the fine structure in the Coulomb-blockade regime but may be used to advantage for the generation of spin-polarized currents.

II. MODEL AND METHODS

For the most part, we consider a monolayer of magnetic molecules sandwiched between two metallic electrodes, see Fig. 1. We assume that magnetic interac-

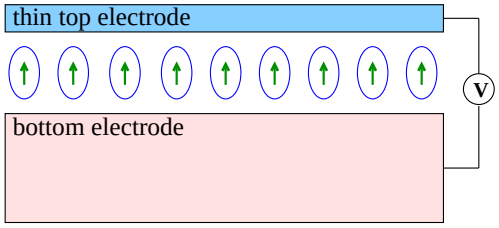

FIG. 1: Sketch of the geometry. A monolayer of magnetic molecules is adsorbed on a metallic substrate, which serves as a bottom electrode. A thin metallic layer is used as a top electrode.

tions between the molecules are negligible and that all molecules have the same spatial orientation relative to the electrodes.[29] In this case it is sufficient to consider the properties of a single molecule. Relaxation in the leads is assumed to be fast so that their electron distributions can be described by equilibrium Fermi functions. In the simplest case, transport involves tunneling through only a single molecular level with onsite energy ϵ_d and local Coulomb repulsion U. The full Hamiltonian of the system reads $H = H_{\rm mol} + H_{\rm leads} + H_{\rm t}$, where[18]

$$H_{\rm mol} = \epsilon_d\, n_d + \frac{U}{2} n_d\,(n_d - 1) - J\,\mathbf{s}\cdot\mathbf{S} - K_2 (S^z)^2 - B\,(s^z + S^z) \qquad (1)$$

describes the molecular degrees of freedom, $H_{\rm leads} = \sum_{\alpha={\rm L,R}} \sum_{\mathbf{k}\sigma} \epsilon_{\alpha\mathbf{k}} a^\dagger_{\alpha\mathbf{k}\sigma} a_{\alpha\mathbf{k}\sigma}$ represents the two leads $\alpha = {\rm L, R}$ (left, right), and $H_{\rm t} = \sum_{\alpha={\rm L,R}} t_\alpha \sum_{\mathbf{k}\sigma} (a^\dagger_{\alpha\mathbf{k}\sigma} c_\sigma + c^\dagger_\sigma a_{\alpha\mathbf{k}\sigma})$ describes the tunneling. The tunneling amplitudes t_α are chosen real. The operator $c^\dagger_\sigma$ creates an electron with spin σ on the molecule. $n_d \equiv c^\dagger_\uparrow c_\uparrow + c^\dagger_\downarrow c_\downarrow$ and $\mathbf{s} \equiv \sum_{\sigma\sigma'} c^\dagger_\sigma \boldsymbol{\sigma}_{\sigma\sigma'} c_{\sigma'}/2$ are the corresponding number and spin operator, respectively. The parameter J denotes the exchange interaction between the electrons and a local spin $\mathbf{S}$, where $\mathbf{S}\cdot\mathbf{S} = S(S+1)$. We restrict ourselves to the case of easy-axis anisotropy, $K_2 > 0$. For simplicity we consider identical g factors for $\mathbf{s}$ and $\mathbf{S}$. An external magnetic field B is applied along the easy axis of the molecule, where a factor $g\mu_B$ has been absorbed into B. $a^\dagger_{\alpha\mathbf{k}\sigma}$ creates an electron in lead α with spin σ, momentum $\mathbf{k}$ and energy $\epsilon_{\alpha\mathbf{k}}$.

The leading contribution to the transition rates between molecular many-particle states is of second order in $H_{\rm t}$, corresponding to sequential tunneling. The transition rates can be obtained from Fermi's Golden Rule,[32]

$$\Gamma^{nn'}_\alpha = 2\pi \sum_\sigma t^2_\alpha \nu_{\alpha\sigma} \Big(f(\epsilon_m - \epsilon_n - \mu_\alpha) |C^\sigma_{nm}|^2 + [1 - f(\epsilon_n - \epsilon_m - \mu_\alpha)]\, |C^\sigma_{mn}|^2 \Big). \qquad (2)$$

Here, the eigenstates $|n\rangle$ and $|n'\rangle$ of $H_{\rm mol}$ denote the initial and final state of the molecule, respectively, $\nu_{\alpha\sigma}$ is the density of states of electrons with spin σ in lead α, $f(\epsilon)$ is the Fermi distribution function, μ_α is the chemical potential in lead α, where $\mu_{\rm L} - \mu_{\rm R} = -eV$, and $C^\sigma_{nn'} \equiv \langle n|c_\sigma|n'\rangle$ is the matrix element of the electron annihilation operator between molecular many-particle states. The typical sequential-tunneling rate involving lead α and electrons with spin σ is given by $1/\tau_{\alpha\sigma} = (2\pi\, t^2_\alpha \nu_{\alpha\sigma})^{-1}$.

To go beyond the leading order, the tunneling Hamiltonian is replaced by the T matrix,[32] which is self-consistently given by

$$T = H_{\rm t} + H_{\rm t} \frac{1}{E_i - H_0 + i\eta} T. \qquad (3)$$

Here, E_i is the energy of the initial state $|i\rangle|n\rangle$, where $|i\rangle$ refers to the equilibrium state of the left and right leads (at different chemical potential) and $|n\rangle$ is a molecular state. Furthermore, $H_0 \equiv H_{\rm mol} + H_{\rm leads}$, with the energy of the leads measured relative to equilibrium, and η is a positive infinitesimal ensuring that the Green function in T is retarded. To fourth order, the transition rate from state $|i\rangle|n\rangle$ to $|f\rangle|n'\rangle$ with an electron tunneling from lead α to lead α' is given by

$$\Gamma^{ni;n'f}_{\alpha\alpha'} = 2\pi \left| \langle f|\langle n'|H_{\rm t} \frac{1}{E_i - H_0 + i\eta} H_{\rm t}|n\rangle|i\rangle \right|^2 \times \delta(E_f - E_i). \qquad (4)$$

The energies of the initial state $|n\rangle|i\rangle$ and final state $|n'\rangle|f\rangle = |n'\rangle a^\dagger_{\alpha'\mathbf{k}'\sigma'} a_{\alpha\mathbf{k}\sigma}|i\rangle$ are denoted by E_i and E_f, respectively. We restrict ourselves to the case of infinite U, i.e., double occupancy of the molecule is forbidden. Inserting $H_{\rm t}$ and summing over final lead states yields

$$\Gamma^{nn',00}_{\alpha\alpha'} = 2\pi t^2_\alpha t^2_{\alpha'} \sum_{\sigma\sigma'} \nu_{\alpha\sigma}\nu_{\alpha'\sigma'} \times \int d\epsilon \left| \sum_{n''} \frac{C^{\sigma'}_{n'n''} C^{\sigma *}_{nn''}}{\epsilon + \epsilon_n - \epsilon_{n''} + i\eta} \right|^2 \times f(\epsilon - \mu_\alpha)\,[1 - f(\epsilon + \epsilon_n - \epsilon_{n'} - \mu_{\alpha'})], \qquad (5)$$

$$\Gamma^{nn',11}_{\alpha\alpha'} = 2\pi t^2_\alpha t^2_{\alpha'} \sum_{\sigma\sigma'} \nu_{\alpha\sigma}\nu_{\alpha'\sigma'} \times \int d\epsilon \left| \sum_{n''} \frac{C^{\sigma'}_{n''n} C^{\sigma *}_{n''n'}}{-\epsilon + \epsilon_{n'} - \epsilon_{n''} + i\eta} \right|^2 \times f(\epsilon - \mu_\alpha)\,[1 - f(\epsilon + \epsilon_n - \epsilon_{n'} - \mu_{\alpha'})], \qquad (6)$$

where $\Gamma^{nn',00}_{\alpha\alpha'}$ ($\Gamma^{nn',11}_{\alpha\alpha'}$) denotes the cotunneling rate describing virtual transitions between two empty (singly occupied) molecular states. Here, we have assumed that the density of states in the leads is independent of energy. To the same order in $H_{\rm t}$, one also obtains processes changing the electron number by ± 2. For $U \to \infty$ these pair-tunneling processes[33] are suppressed. Note that Eqs. (5) and (6) contain both elastic and inelastic cotunneling.

Since the above expressions diverge due to second-order poles from the energy denominators, the cotunneling rates cannot be evaluated directly.[34,35,36,37] We

apply a regularization scheme that follows Refs. 35,36,37 and is motivated by the observation that Eqs. (5) and (6) do not take into account that the intermediate state obtains a finite width Γ due to tunneling. In our regime of weak tunneling, the width Γ is of second order in the tunneling amplitudes t_α. This width is introduced into the energy denominators, replacing η. When the cotunneling rates are expanded in powers of Γ, it turns out that the leading term is of order $1/\Gamma \propto 1/t_\alpha^2$. This cancels two powers of the tunneling amplitude in Eqs. (5) and (6) so that the result is in fact a *sequential-tunneling* contribution. Since we have already included the full sequential-tunneling rates, this new contribution should be dropped. We thus take the next order, Γ^0, for the cotunneling rates.

The sequential and cotunneling rates appear in the rate equations for the probabilities to find the molecule in state $|n\rangle$,

$$\frac{dP^n}{dt} = \sum_{\alpha m} \left(\Gamma_\alpha^{mn} P^m - \Gamma_\alpha^{nm} P^n\right) + \sum_{\alpha\alpha' m} \left(\Gamma_{\alpha\alpha'}^{mn} P^m - \Gamma_{\alpha\alpha'}^{nm} P^n\right), \tag{7}$$

where $\Gamma_{\alpha\alpha'}^{mn} \equiv \Gamma_{\alpha\alpha'}^{mn,00} + \Gamma_{\alpha\alpha'}^{mn,11}$ and $\Gamma_{\alpha\alpha'}^{mn,00}$ ($\Gamma_{\alpha\alpha'}^{mn,11}$) is non-zero only if both $|n\rangle$ and $|m\rangle$ are empty (singly occupied). The current through the left lead is given by

$$I^{\rm L} = -e\sum_{nm}(n_n - n_m)\Gamma_{\rm L}^{mn} P^m - e\sum_{nm}(\Gamma_{\rm LR}^{mn} - \Gamma_{\rm RL}^{mn})\, P^m. \tag{8}$$

The *steady-state* probabilities P^m of molecular states are obtained by solving Eq. (7) with the time derivatives set to zero. The average magnetization in the z direction per molecule is given by $M = \sum_n m_n P^n$, where m_n denotes the quantum number of the z component of the total spin $\mathbf{s} + \mathbf{S}$ in state $|n\rangle$.

III. RESULTS AND DISCUSSION

We start by discussing the results obtained for the differential conductance dI/dV at low bias voltages. If the system is in the Coulomb-blockade regime, sequential tunneling is thermally suppressed and transport is dominated by cotunneling. The magnitude of the current is then small. The conductance at zero bias voltage is finite, see Fig. 2(a), due to *elastic* cotunneling. The cotunneling rates are proportional to the bias voltage, if the molecular level is far from the chemical potentials, leading to ohmic behavior. The rounded steps in dI/dV correspond to the onset of additional *inelastic* cotunneling processes. Selection rules for the spin quantum number require $\Delta m = 0, \pm 1$. For the parameters chosen in Fig. 2, the ground state has electron number $n = 1$ and maximum spin, $m = 5/2$. Inelastic cotunneling processes corresponding to the two steps involve the two different final states with $n = 1$, $m = 3/2$ and virtual occupation

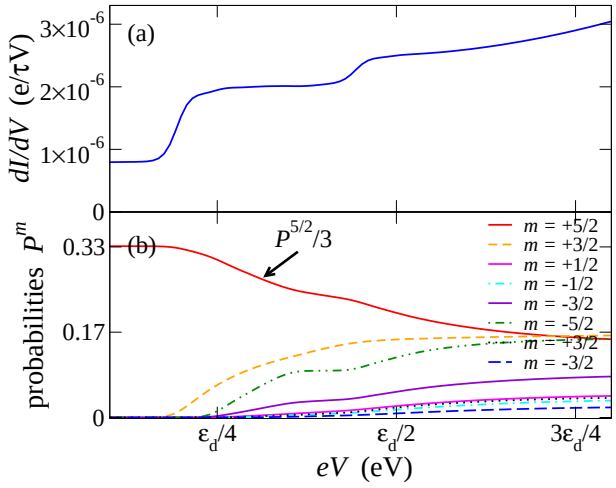

FIG. 2: (Color online) (a) Differential conductance dI/dV and (b) probabilities P^n of molecular many-particle states as functions of bias voltage V, for low bias voltages. The probability $P^{5/2}$ of the ground state has been scaled by a factor 1/3. Here, we assume $S = 2$, $J = K_2 = 5\,$meV, $\epsilon_d = 10\,J$, $B = 2\,$meV, and $T = 0.3\,$meV.

of the state with $n = 0$, $m = 2$, as illustrated in Fig. 3. Further steps in dI/dV are not observed, since the corresponding inelastic cotunneling transitions have smaller energy differences between initial and final states and are therefore activated immediately when the probability of the initial state becomes significant.

Cotunneling steps and sequential tunneling peaks show fundamentally different dependences on the onsite energy ϵ_d. For *single-molecule* junctions it is possible to change ϵ_d by applying a gate voltage, e.g., in break-junction experiments. For monolayers one does not have this opportunity. We come back to this point below. While the bias voltages at which sequential tunneling peaks occur shift linearly with ϵ_d, the positions of cotunneling steps remain unaffected. This follows directly from evaluating Eqs. (5)–(6) in the limit of large ϵ_d.[32] For magnetic molecules, the position of the cotunneling steps shifts linearly as a function of the external magnetic field due to the Zeeman effect, as observed for Mn_{12}.[17]

While dI/dV represents the change of the *very small* current with bias voltage in the cotunneling regime, the change of the probabilities P^n of molecular states with bias voltage is of order unity, as shown in Fig. 2(b). The probability of the lowest-energy state with $m = 5/2$ decreases, whereas the probabilities of other states increase. Cotunneling enables transitions between molecular states with the same electron number but with magnetic quantum numbers differing by $\Delta m = \pm 1$. These transitions are suppressed only as the inverse square of the energy difference between the initial state and the virtual state involved. In sequential tunneling, such transitions are also possible, requiring two consecutive steps, but are *exponentially* suppressed in the Coulomb-blockade regime.

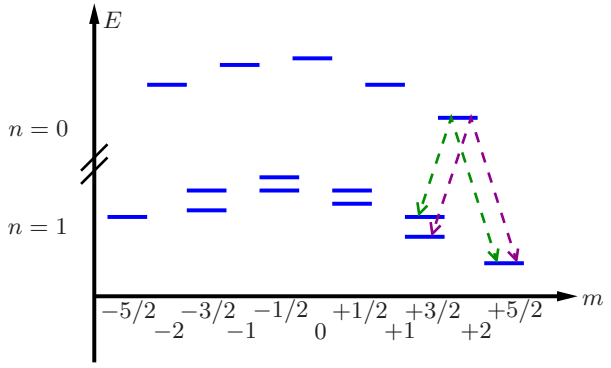

FIG. 3: Level scheme showing the energies of molecular states as a function of magnetic quantum number m for electron numbers $n = 0, 1$. The dashed double arrows signify inelastic cotunneling between the ground state with $m = 5/2$ and the two states with $m = 3/2$, involving virtual occupation of the state with $n = 0$ and $m = 2$. While sequential tunneling requires a change of the electron number by $\Delta n = \pm 1$ and of the magnetic quantum number by $\Delta m = \pm 1/2$, cotunneling processes obey the selection rules $\Delta n = 0$, $\Delta m = 0, \pm 1$.

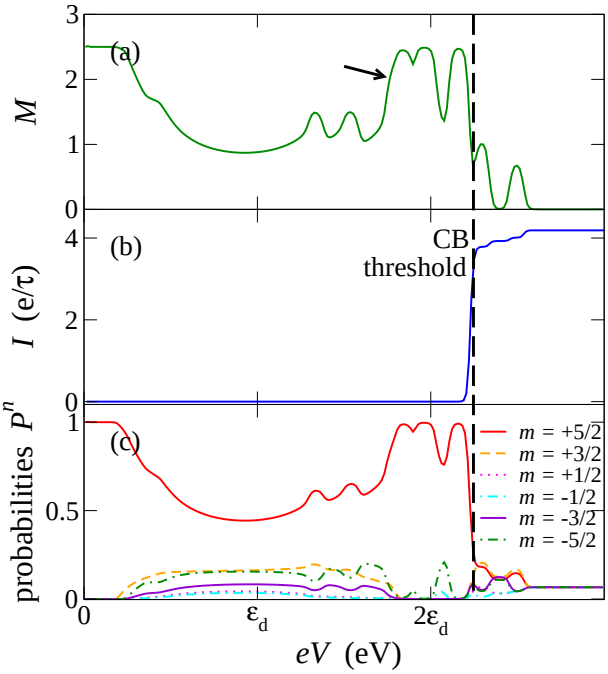

FIG. 4: (Color online) (a) Magnetization M, (b) current I, and (c) probabilities P^n of various molecular many-particle states as functions of bias voltage V. The parameters are chosen as in Fig. 2.

In the sequential-tunneling approximation the molecule would thus remain in the lowest-energy state with essentially unit probability. This approximation is evidently invalid for determining the probabilities in this regime.

Interestingly, the strong effect of cotunneling on the probabilities also leads to observable effects of *sequential* tunneling on transport in the cotunneling regime.[37,38] While sequential tunneling starting from the lowest-energy state is exponentially suppressed, sequential tunneling from higher-energy states can be possible. With increasing bias voltage, these higher-energy states become increasingly populated due to *cotunneling*, as Fig. 2(b) shows. This leads to sidebands in dI/dV in the Coulomb-blockade regime that show the linear dependence on the gate voltage characteristic of sequential tunneling.[37] Strong electron-phonon coupling can enhance this effect, since it crucially affects the ratio of the rates for sequential and cotunneling processes.[37] In our case, these sidebands are very weak, since the current is controlled by the small cotunneling rates. However, we will see that the effect on the *probabilities* P^n of molecular states is significant.

Figure 4(a) shows the average magnetization per molecule as a function of bias voltage over a broad voltage range including both the cotunneling and sequential tunneling regimes. The magnetization is nonzero since our model contains an external magnetic field. At zero bias, the molecule is in its ground state with $m = 5/2$. The onset of inelastic cotunneling to the two states with $m = 3/2$ leads to a decrease in the magnetization in each case.

The bias-voltage dependence of the magnetization for voltages *above* the Coulomb blockade threshold is accompanied by sizeable steps in the current, as seen in Fig. 4(b). At each of these fine-structure steps an additional inelastic sequential-tunneling transition becomes possible. The Coulomb-blockade threshold corresponds to the transition with initial state $n = 1$, $m = 5/2$ and final state $n = 0$, $m = 2$. Therefore, the onset of sequential tunneling is accompanied by a *decrease* in the magnetization. At large bias the magnetization drops to zero since all states are occupied with equal probability.

Remarkably, pronounced step-like features are also present *below* the Coulomb-blockade threshold in Fig. 4(a). This can be understood from the bias-voltage dependence of the relevant probabilities P^n in Fig. 4(c). As an example, consider the step marked by an arrow in Fig. 4(a). The physics leading to the drastic change of the probabilities is illustrated in Fig. 5: The sequential tunneling processes with $m = -3/2 \to -2$, $m = -1/2 \to -1$, $m = 3/2 \to 2$, and $m = 1/2 \to 1$, starting at the higher-energy level of each pair (thin arrows in Fig. 5), are already energetically possible at lower bias voltages causing the partial depopulation of the initial states. However, the probabilities of these states are non-zero mainly due to cotunneling processes (dashed arrows in Fig. 5). Below the step marked in Fig. 4(a), the half-integer spin states with positive and negative m are *not connected* by sequential tunneling processes. As soon as the transition with $m = -1/2 \to 0$ (bold arrow in Fig. 5) becomes possible, the states with positive and negative m are connected and fast, sequential tunneling processes depopulate all states except for the

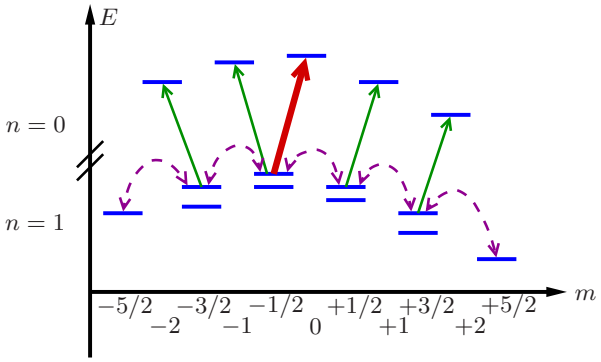

FIG. 5: Level scheme illustrating the interplay between sequential tunneling (solid arrows) and cotunneling (dashed arrows) in magnetic molecules. Even below the Coulomb-blockade threshold sequential tunneling processes starting from higher-energy states populated by cotunneling may cause the depopulation of these states and drastically affect the average magnetization. At the step denoted by an arrow in Fig. 4(a), the excitation of the transition with $m = -1/2 \to 0$ (heavy solid arrow) gives rise to a redistribution of the probabilities P^n. Note that exothermal transitions with $\Delta m = \pm 1/2$ are always possible.

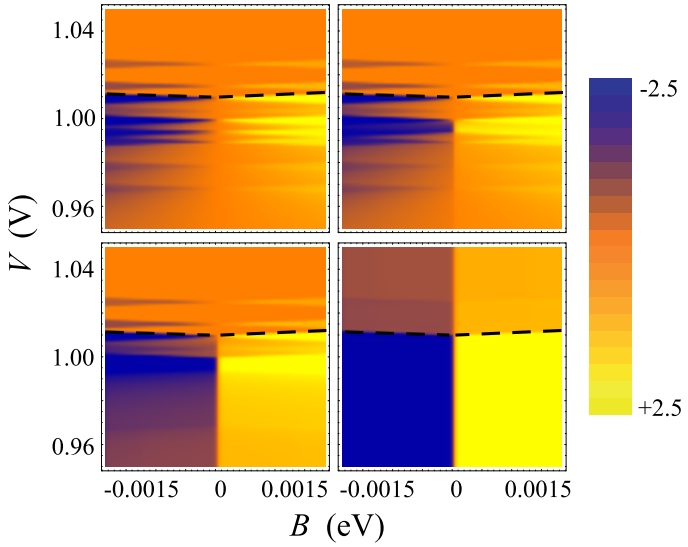

FIG. 6: (Color online) Magnetization M as a function of bias voltage V and magnetic field B for different spin relaxation times: (a) $t_{\rm rel} = 10^{10}\tau$, (b) $t_{\rm rel} = 10^{6}\tau$, (c) $t_{\rm rel} = 10^{4}\tau$, and (d) $t_{\rm rel} = \tau$. Here $\tau = 2\pi t_\alpha^2 \nu_\alpha$ denotes the typical electronic tunneling time, assuming symmetric coupling to the leads. All other parameters are chosen as above. The dashed lines denote the Coulomb-blockade threshold.

ground state, which has $m = 5/2$. Consequently, the average magnetization again approaches its maximum value. Similarly, one can attribute each step to a particular molecular transition.

The above discussion shows that quantities that depend strongly on the probabilities of molecular states, such as the magnetization, are much more sensitive to changes of the bias voltage in the Coulomb-blockade regime than the conductivity. This suggests to use the *magnetization-voltage* characteristics, i.e., the magnetization as a function of bias voltage, instead of the current-voltage characteristics to extract the excitation spectrum of magnetic molecules. In order to distinguish magnetic transitions from, e.g., vibrational excitations, one should analyze their dependence on the magnetic field. In addition, for a monolayer there is no gate voltage that can serve as an independent parameter. The magnetic field can assume this role.

Figure 6(a) shows a density plot of the magnetization as a function of bias voltage and magnetic field. The magnetization is obviously an odd function of the field. The transition energies shift linearly with the field, $\Delta E = \Delta m\, B$, if the initial and final states have different magnetic quantum numbers m.

Complementary to the conventional differential-conductance plots, the density plots in Fig. 6 can serve as fingerprints of the internal degrees of freedom of the molecules. The Zeeman splitting of the molecular levels due to the external magnetic field gives rise to triangular plateaus with a tip at $B = 0$. These plateaus are bounded by two molecular transitions involving sequential tunneling. In each case, these two transitions differ in the sign of the magnetic quantum number m of both initial and final molecular states. For the chosen parameters, the plateaus can be attributed to the following transitions from empty to singly occupied states, starting at low bias voltage (cf. Fig. 5): $|m| = 3/2 \to 2$, $|m| = 1/2 \to 1$, $|m| = 1/2 \to 0$, $|m| = 3/2 \to 2$, $|m| = 3/2 \to 1$, $|m| = 1/2 \to 1$, $|m| = 5/2 \to 2$ (this is the first transition starting from the ground state and thus represents the Coulomb-blockade threshold), $|m| = 1/2 \to 0$, and $|m| = 3/2 \to 1$. Several transitions appear twice because there are two states with magnetic quantum numbers $\pm 3/2$ and $\pm 1/2$, respectively. For a local spin $S = 2$ there exist nine transitions obeying the selection rule $\Delta m = \pm 1/2$, as can be seen from Fig. 5, in accordance with the nine plateaus shown in Fig. 6(a). Note again that the signal is similar on both sides of the Coulomb-blockade threshold.

So far we have restricted ourselves to the situation where the relaxation of the local molecular spin is dominated by electron tunneling, i.e., the spin is *conserved* between tunneling events. However, there are other processes that also contribute to spin relaxation: (i) Magnetic molecules containing transition-metal ions, such as Mn_{12} clusters, show strong spin-orbit interaction, which leads to spin relaxation. (ii) Hyperfine interactions with nuclear magnetic moments in the molecule can also lead to spin relaxation. However, in molecules one has the chance to essentially remove this mechanism by choosing isotopes with vanishing nuclear spins. (iii) Dipolar inter-

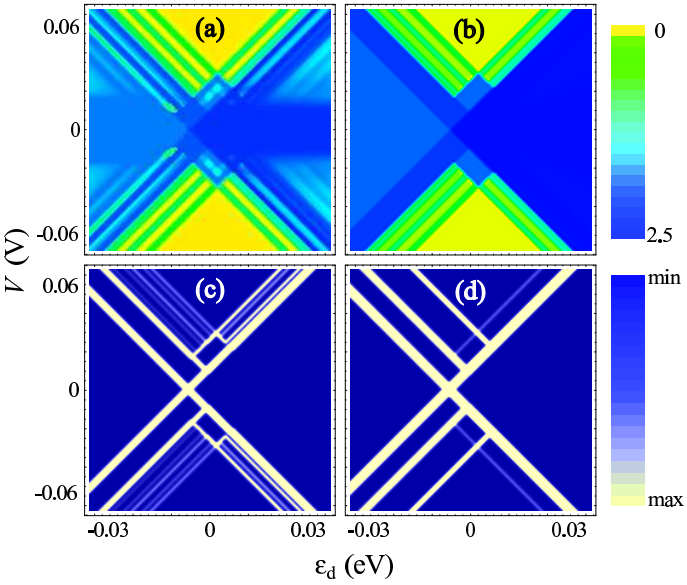

FIG. 7: (Color online) (a), (b) Magnetization M and (c), (d) differential conductance of a single magnetic molecule as a function of V and ϵ_d for (a), (c) slow spin relaxation, $t_{\rm rel} = 10^{10}\tau$, and (b), (d) fast spin relaxation, $t_{\rm rel} = \tau$. We assume $S = 2$, $J = K_2 = 5\,$meV, $T = 0.1\,$meV, and $B = 2\,$meV. $\tau = 2\pi t_\alpha^2 \nu_\alpha$ is the typical tunneling time, assuming symmetric coupling to the leads.

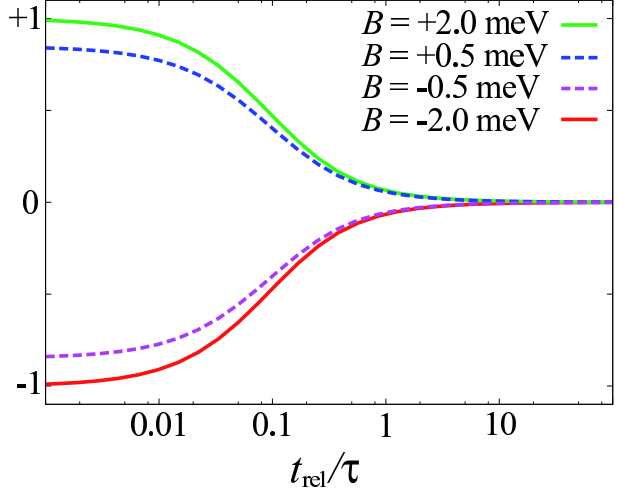

FIG. 8: (Color online) Polarization of the current, $p \equiv (I^{\rm L\uparrow} - I^{\rm L\downarrow})/(I^{\rm L\uparrow} + I^{\rm L\downarrow})$, as a function of spin relaxation time $t_{\rm rel}$ in units of the typical tunneling time τ.

actions with spins of other molecules in the monolayer or with impurity spins in the electrodes contribute to spin relaxation. (iv) Small non-uniaxial magnetic anisotropies lead to tunneling between the eigenstates of $H_{\rm mol}$. This mechanism has recently been discussed in the context of transport through magnetic molecules.[14,15,16]

All these processes change the magnetic quantum number while keeping the electron number constant ($\Delta n = 0$). The dominant transitions are the ones with $\Delta m = \pm 1$. These are the same selection rules as for cotunneling, indicating that one should include additional spin relaxation for consistency when studying cotunneling.

The effect of spin relaxation on the electronic transport is included in the formalism by a phenomenological rate $\propto 1/t_{\rm rel}$ which forces the system to approach the equilibrium distribution on the timescale $t_{\rm rel}$. We include additional transition rates between states $|n\rangle$ and $|m\rangle$ with $\Delta n = 0$ and $\Delta m = \pm 1$, $\Gamma^{\rm rel}_{nm} = \exp[(\epsilon_n - \epsilon_m)/kT]/t_{\rm rel}$ for $\epsilon_n < \epsilon_m$ and $\Gamma^{\rm rel}_{nm} = 1/t_{\rm rel}$ otherwise. The additional rates obey detailed balance, ensuring relaxation towards equilibrium in the absence of tunneling.

Effects of spin relaxation on the bias-voltage dependence of the magnetization are illustrated in Figs. 6(a)–(d). For small $t_{\rm rel}$ (fast relaxation), the number of transitions appearing as steps in the magnetization-voltage characteristics is reduced, since spin relaxation depopulates higher-energy states that serve as initial states for these transitions.

So far we have considered a monolayer of magnetic molecules, mostly because the measurement of the magnetization is easier for larger numbers of molecules. As mentioned previously, even the detection of a *single* molecular spin might be feasible.[27,28] Using a single molecule allows one to introduce a gate electrode in order to tune the molecular energy levels by shifting ϵ_d, see Eq. (1). In the following, we briefly discuss results obtained for varying gate voltage. To increase the magnetization signal while retaining the gate electrode, one might consider a one-dimensional array of magnetic molecules or even a large number of such arrays aligned in parallel.

The plot of the magnetization and the differential conductance as functions of bias voltage and onsite energy ϵ_d presented in Figs. 7(a),(c) shows two striking features. First, the magnetization shows steps indicating the onset of inelastic cotunneling which are almost independent of ϵ_d. The corresponding steps in dI/dV are very small in absolute units, see Fig. 2(a).

Second, the magnetization shows strong additional magnetic sidebands in the Coulomb-blockade regime. These sidebands are the consequence of sequential-tunneling transitions depopulating molecular states that are populated by cotunneling, as discussed above. In dI/dV the corresponding features are completely hidden by the low-bias tail of the large peak at the Coulomb-blockade threshold (not shown). The observation of these sidebands in the Coulomb-blockade regime requires spin relaxation times long compared to the typical tunneling time. For fast spin relaxation, fine-structure peaks are only present in the sequential-tunneling regime, see Fig. 7(b), since sequential tunneling is still faster than spin relaxation, even though cotunneling is slower. As shown in Fig. 7(d), the absence of such sidebands is accompanied by suppressed fine-structure peaks in the sequential-tunneling regime.

Finally, we note that sufficiently fast spin relaxation

leads to *spin-polarized* stationary currents in the presence of a magnetic field. If the spin of the magnetic molecule relaxes fast compared to the typical tunneling rate, which is essentially determined by the current, the system is essentially always in its ground state. Due to the Zeeman effect the ground state has maximum magnetic quantum number; $m = 5/2$ for our example. Thus only spin-down electrons can tunnel onto the molecule, resulting in a spin-polarized current. Note that this argument is not restricted to low-order perturbation theory in H_t. As shown in Fig. 8, the degree of spin polarization is basically determined by the ratio of the spin relaxation rate and the typical electronic tunneling rate.

IV. CONCLUSIONS

In summary, we have studied the interplay of electronic transport through magnetic molecules and their nonequilibrium magnetic moment beyond the sequential-tunneling approximation. We have focused mostly on monolayers, which should give a better chance to measure the magnetization than single molecules would.

While the excitation of inelastic tunneling processes in the Coulomb-blockade regime leads only to a very small absolute change in the current, the change of the probabilities to find the molecule in various many-particle states is significant. This manifests itself in a strong bias-voltage dependence of the magnetization. The magnetization of a molecular monolayer can be switched by an amount of the order of the saturation magnetization by a small change of bias voltage, and without causing the flow of a large current.

We find steps in the differential conductance due to inelastic cotunneling, which have been observed in experiments on Mn_{12}.[17] These steps are accompanied by much larger changes in the magnetization. Another interesting effect is the appearance of additional sidebands in the Coulomb-blockade regime that can be ascribed to *de*-excitations by sequential tunneling of states populated by cotunneling. These sidebands are very prominent in the magnetization. We suggest that the magnetization, or any measurable quantity that strongly differs between molecular states, can be employed to study molecular transitions that are, from the point of view of transport, hidden in the Coulomb-blockade regime.

For spintronics applications, the ability to control the persistence of the stored information is crucial. In this context, we have considered effects of additional spin relaxation in the same formalism. Our results show that for sufficiently fast spin relaxation the peaks in the differential conductance and the steps in the magnetization are washed out, as expected. At the same time, the degree of polarization of the steady-state current contains information about the ratio of the spin relaxation rate and the typical electronic tunneling rate. Fast spin relaxation, while in general undesirable, can lead to a highly polarized current in the presence of a magnetic field.

Acknowledgments

We would like to thank J. Koch and F. von Oppen for valuable discussions. Support by the Deutsche Forschungsgemeinschaft through Sonderforschungsbereich 658 is gratefully acknowledged.

* Electronic address: felste@physik.fu-berlin.de
† Electronic address: ctimm@ku.edu

[1] S. A. Wolf, D. D. Awschalom, R. A. Buhrman, J. M. Daughton, S. von Molnár, M. L. Roukes, A. Y. Chtchelkanova, and D. M. Treger, Science **294**, 1488 (2001).
[2] I. Žutić, J. Fabian, and S. Das Sarma, Rev. Mod. Phys. **76**, 323 (2004).
[3] S. Sanvito and A. R. Rocha, J. Comput. Theor. Nanosci. **3**, 624 (2006).
[4] E. G. Emberly and G. Kirczenow, Chem. Phys. **281**, 311 (2002); Phys. Rev. Lett. **91**, 188301 (2003).
[5] A. Nitzan and M. A. Ratner, Science **300**, 1384 (2003).
[6] Y. Xue and M. A. Ratner, Phys. Rev. B **68**, 115406 (2003); Phys. Rev. B **68**, 115407 (2003); in *Nanotechnology: Science and Computation*, edited by J. Chen, N. Jonoska, and G. Rozenberg (Springer-Verlag, Berlin, 2006).
[7] C. Joachim, J. K. Gimzewski, and A. Aviram, Nature (London) **408**, 541 (2000).
[8] W. Harneit, Phys. Rev. A **65**, 032322 (2002).
[9] S. J. Blundell and F. L. Pratt, J. Phys.: Condens. Matter **16**, R771 (2004).
[10] J. Park, A. N. Pasupathy, J. I. Goldsmith, C. Chang, Y. Yaish, J. R. Petta, M. Rinkoski, J. P. Sethna, H. D. Abruña, P. L. McEuen, and D. C. Ralph, Nature (London) **417**, 722 (2002).
[11] W. Liang, M. P. Shores, M. Bockrath, J. R. Long, and H. Park, Nature (London) **417**, 725 (2002).
[12] J. Paaske and K. Flensberg, Phys. Rev. Lett. **94**, 176801 (2005).
[13] F. Elste and C. Timm, Phys. Rev. B **71**, 155403 (2005).
[14] C. Romeike, M. R. Wegewijs, W. Hofstetter, and H. Schoeller, Phys. Rev. Lett. **96**, 196601 (2006).
[15] C. Romeike, M. R. Wegewijs, and H. Schoeller, Phys. Rev. Lett. **96**, 196805 (2006).
[16] H. B. Heersche, Z. de Groot, J. A. Folk, H. S. J. van der Zant, C. Romeike, M. R. Wegewijs, L. Zobbi, D. Barreca, E. Tondello, and A. Cornia, Phys. Rev. Lett. **96**, 206801 (2006).
[17] M.-H. Jo, J. E. Grose, K. Baheti, M. M. Deshmukh, J. J. Sokol, E. M. Rumberger, D. N. Hendrickson, J. R. Long, H. Park, and D. C. Ralph, Nano Lett. **6**, 2014 (2006).
[18] C. Timm and F. Elste, Phys. Rev. B **73**, 235304 (2006).
[19] F. Elste and C. Timm, Phys. Rev. B **73**, 235305 (2006).
[20] M. N. Leuenberger and E. R. Mucciolo, Phys. Rev. Lett.

97, 126601 (2006).
[21] A. Donarini, M. Grifoni, and K. Richter, Phys. Rev. Lett. **97**, 166801 (2006).
[22] C. Romeike, M. R. Wegewijs, W. Hofstetter, and H. Schoeller, cond-mat/0605514 (unpublished).
[23] M. Misiorny and J. Barnas, cond-mat/0610556 (unpublished).
[24] G. Gonzalez and M. N. Leuenberger, cond-mat/0610653 (unpublished).
[25] J. J. Parks, A. R. Champagne, G. R. Hutchison, S. Flores-Torres, H. D. Abruña, and D. C. Ralph, cond-mat/0610555 (unpublished).
[26] M. Zomack and K. Baberschke, Surf. Sci. **178**, 618 (1986); Phys. Rev. B 36, R5756 (1987).
[27] C. Durkan and M. E. Welland, Appl. Phys. Lett. **80**, 458 (2002).
[28] D. Rugar, R. Budakian, H. J. Mamin, and B. W. Chui, Nature (London) **430**, 329 (2004).
[29] C. Zhou, M. R. Deshpande, M. A. Reed, L. Jones, II., and J. M. Tour, Appl. Phys. Lett. **71**, 611 (1997).
[30] A. Mitra, I. Aleiner, and A. J. Millis, Phys. Rev. B **69**, 245302 (2004).
[31] K. Blum, *Density Matrix Theory and Applications* (Plenum, New York, 1981).
[32] H. Bruus and K. Flensberg, *Many-body Quantum Theory in Condensed Matter Physics* (Oxford University Press, Oxford, 2004).
[33] J. Koch, M. E. Raikh, and F. von Oppen, Phys. Rev. Lett. **96**, 056803 (2006).
[34] D. V. Averin, Physica B **194–196**, 979 (1994).
[35] M. Turek and K. A. Matveev, Phys. Rev. B **65**, 115332 (2002).
[36] J. Koch, F. von Oppen, Y. Oreg, and E. Sela, Phys. Rev. B **70**, 195107 (2004).
[37] J. Koch, F. von Oppen, and A. V. Andreev, cond-mat/0606512 (unpublished).
[38] B. LeRoy, S. Lemay, J. Kong, and C. Dekker, Nature (London) **432**, 371 (2004).